

Haverford College

Haverford Scholarship

Faculty Publications

Physics

2011

Arecibo PALFA Survey and Einstein@Home: Binary Pulsar Discovery by Volunteer Computing

Benjamin Knispel

Patile Lazarus

Bruce Allen

David Anderson

Fronefield Crawford

Haverford College, fcrawford@haverford.edu

Follow this and additional works at: https://scholarship.haverford.edu/physics_facpubs

Repository Citation

"Arecibo PALFA Survey and Einstein@Home: Binary Pulsar Discovery by Volunteer Computing" B. Knispel, P. Lazarus, B. Allen, D. Anderson, C. Aulbert, N. D. R. Bhat, O. Bock, S. Bogdanov, A. Brazier, F. Camilo, S. Chatterjee, J. M. Cordes, F. Crawford, J. S. Deneva, G. Desvignes, H. Fehrmann, P. C. C. Freire, D. Hammer, J. W. T. Hessels, F. A. Jenet, V. M. Kaspi, M. Kramer, J. van Leeuwen, D. R. Lorimer, A. G. Lyne, B. Machenschalk, M. A. McLaughlin, C. Messenger, D. J. Nice, M. A. Papa, H. J. Pletsch, R. Prix, S. M. Ransom, X. Siemens, I. H. Stairs, B. W. Stappers, K. Stovall, & A. Venkataraman, *Astrophysical Journal Letters*, 732, L1 (2011).

This Journal Article is brought to you for free and open access by the Physics at Haverford Scholarship. It has been accepted for inclusion in Faculty Publications by an authorized administrator of Haverford Scholarship. For more information, please contact nmedeiro@haverford.edu.

ARECIBO PALFA SURVEY AND EINSTEIN@HOME: BINARY PULSAR DISCOVERY BY VOLUNTEER COMPUTING

B. KNISPEN^{1,2}, P. LAZARUS³, B. ALLEN^{1,2,4}, D. ANDERSON⁵, C. AULBERT^{1,2}, N. D. R. BHAT⁶, O. BOCK^{1,2}, S. BOGDANOV³, A. BRAZIER^{7,8}, F. CAMILO⁹, S. CHATTERJEE⁷, J. M. CORDES⁷, F. CRAWFORD¹⁰, J. S. DENEVA¹¹, G. DESVIGNES¹², H. FEHRMANN^{1,2}, P. C. C. FREIRE¹³, D. HAMMER⁴, J. W. T. HESSELS^{14,15}, F. A. JENET¹⁶, V. M. KASPI³, M. KRAMER^{13,17}, J. VAN LEEUWEN^{14,15}, D. R. LORIMER^{18,24}, A. G. LYNE¹⁷, B. MACHENSCHALK^{1,2}, M. A. McLAUGHLIN^{18,24}, C. MESSENGER^{1,2,19}, D. J. NICE²⁰, M. A. PAPA^{4,21}, H. J. PLETSCH^{1,2}, R. PRIX^{1,2}, S. M. RANSOM²², X. SIEMENS⁴, I. H. STAIRS²³, B. W. STAPPERS¹⁷, K. STOVALL¹⁶,
AND A. VENKATARAMAN¹¹

¹ Albert-Einstein-Institut, Max-Planck-Institut für Gravitationsphysik, D-30167 Hannover, Germany

² Institut für Gravitationsphysik, Leibniz Universität Hannover, D-30167 Hannover, Germany

³ Department of Physics, McGill University, Montreal, QC H3A2T8, Canada

⁴ Physics Department, University of Wisconsin-Milwaukee, Milwaukee, WI 53211, USA

⁵ Space Science Laboratory, University of California at Berkeley, Berkeley, CA 94720, USA

⁶ Swinburne University, Center for Astrophysics and Supercomputing, Hawthorn, Victoria 3122, Australia

⁷ Astronomy Department, Cornell University, Ithaca, NY 14853, USA

⁸ NAIC, Cornell University, Ithaca, NY 14853, USA

⁹ Columbia Astrophysics Laboratory, Columbia University, New York, NY 10027, USA

¹⁰ Department of Physics and Astronomy, Franklin and Marshall College, Lancaster, PA 17604-3003, USA

¹¹ Arecibo Observatory, HC3 Box 53995, Arecibo, PR 00612, USA

¹² Department of Astronomy and Radio Astronomy Laboratory, University of California, Berkeley, CA 94720, USA

¹³ Max-Planck-Institut für Radioastronomie, D-53121 Bonn, Germany

¹⁴ Netherlands Institute for Radio Astronomy (ASTRON), Postbus 2, 7990 AA Dwingeloo, The Netherlands

¹⁵ Astronomical Institute "Anton Pannekoek," University of Amsterdam, 1098 SJ Amsterdam, The Netherlands

¹⁶ Center for Gravitational Wave Astronomy, University of Texas-Brownsville, TX 78520, USA

¹⁷ Jodrell Bank Centre for Astrophysics, School of Physics and Astronomy, University of Manchester, Manchester M13 9PL, UK

¹⁸ Department of Physics, West Virginia University, Morgantown, WV 26506, USA

¹⁹ Cardiff School of Physics and Astronomy, Cardiff University, Queens Buildings, The Parade, Cardiff, CF24 3AA, UK

²⁰ Department of Physics, Lafayette College, Easton, PA 18042, USA

²¹ Albert-Einstein-Institut, Max-Planck-Institut für Gravitationsphysik, D-14476 Golm, Germany

²² NRAO (National Radio Astronomy Observatory), Charlottesville, VA 22903, USA

²³ Department of Physics and Astronomy, University of British Columbia, Vancouver, BC V6T 1Z1, Canada

Received 2011 February 25; accepted 2011 March 15; published 2011 April 6

ABSTRACT

We report the discovery of the 20.7 ms binary pulsar J1952+2630, made using the distributed computing project Einstein@Home in Pulsar ALFA survey observations with the Arecibo telescope. Follow-up observations with the Arecibo telescope confirm the binary nature of the system. We obtain a circular orbital solution with an orbital period of 9.4 hr, a projected orbital radius of 2.8 lt-s, and a mass function of $f = 0.15 M_{\odot}$ by analysis of spin period measurements. No evidence of orbital eccentricity is apparent; we set a 2σ upper limit $e \lesssim 1.7 \times 10^{-3}$. The orbital parameters suggest a massive white dwarf companion with a minimum mass of $0.95 M_{\odot}$, assuming a pulsar mass of $1.4 M_{\odot}$. Most likely, this pulsar belongs to the rare class of intermediate-mass binary pulsars. Future timing observations will aim to determine the parameters of this system further, measure relativistic effects, and elucidate the nature of the companion star.

Key words: pulsars: general – pulsars: individual (J1952+2630) – stars: neutron – white dwarfs

1. INTRODUCTION

Pulsars in short-period orbits with neutron stars or white dwarfs are invaluable tools for diverse areas of science. Pulsars are precise clocks and enable very stringent tests of Einstein's theory of general relativity (e.g., Taylor & Weisberg 1989; Kramer & Wex 2009). These binary systems also provide unique opportunities to studying their properties as stellar-evolution endpoints (see review by Stairs 2004). The detection of relativistic effects like the Shapiro delay, most easily measured for highly inclined binary systems with a massive companion, can reveal the orbital geometry as well as the masses of the pulsar and its companion (Ferdman et al. 2010). Precise mass measurements of the pulsar further our understanding of matter

at (super)nuclear densities by providing constraints on the possible equations of state, e.g., Demorest et al. (2010).

Here, we report the discovery and the orbital parameters of PSR J1952+2630. This pulsar is in an almost circular 9.4 hr orbit with a massive companion of at least $0.95 M_{\odot}$, assuming a pulsar mass of $1.4 M_{\odot}$. Thus, this new binary system is a good candidate for the measurement of relativistic effects like the Shapiro delay and could have an impact on all science areas listed above.

2. DISCOVERY OF PSR J1952+2630

PSR J1952+2630 was discovered in Pulsar ALFA (PALFA) survey observations taken in 2005 August with the 305 m Arecibo telescope. The survey observations cover two sky regions close to the Galactic plane ($|b| \leq 5^{\circ}$). One region is in the inner Galaxy ($32^{\circ} \lesssim \ell \lesssim 77^{\circ}$) and is observed with

²⁴ Also adjunct at the NRAO (National Radio Astronomy Observatory), Green Bank, WV 24944, USA.

268 s dwell time per observation; the other in the outer Galaxy ($168^\circ \lesssim \ell \lesssim 214^\circ$) with 134 s long observations. The observations use ALFA, a cooled seven feed-horn, dual-polarization receiver at 1.4 GHz (Cordes et al. 2006). Signals are amplified, filtered, and down-converted. Then, autocorrelation spectrometers, the Wideband Arecibo Pulsar Processors (WAPPs; Dowd et al. 2000), sum polarizations and generate spectra over 100 MHz of bandwidth with 256 channels every $64 \mu\text{s}$.

Data are archived at the Center for Advanced Computing (CAC), Cornell University. They are searched for isolated and binary pulsars in three independent pipelines: (1) a pipeline at the CAC searching for isolated pulsars and single pulses; (2) a pipeline using the PRESTO²⁵ software package operating at several PALFA Consortium member sites, searching for isolated pulsars and binary pulsars with orbits longer than ≈ 1 hr, and single pulses; and (3) Einstein@Home, searching for isolated or binary pulsars with orbits longer than 11 minutes.

Einstein@Home²⁶ is a distributed computing project. Its main goal is the detection of gravitational waves from unknown rapidly spinning neutron stars in data from the LIGO and VIRGO detectors (Abbott et al. 2009). Since 2009 March, about 35% of Einstein@Home compute cycles have been used to search for pulsars in radio data from the PALFA survey. For Einstein@Home, volunteer members of the public sign up their home or office computers, which automatically download work units from project servers over the internet, carry out analyses when idle, and return results. These are automatically validated by comparison with results for the *same* work unit, produced by a different volunteer's computer. As of today, more than 280,000 individuals have contributed; each week about 100,000 different computers download work. The aggregate sustained computational power of $0.38 \text{ PFlop s}^{-1}$ is comparable to that of the world's largest supercomputers.²⁷

For Einstein@Home, raw data are transferred from the CAC to the Albert Einstein Institute, Hannover, Germany, via high-speed internet connections. There, servers dedisperse the raw data into time series with 628 trial dispersion measure (DM) values up to $1002.4 \text{ pc cm}^{-3}$. For bandwidth and throughput reasons, the time resolution of the raw data is reduced by a factor of two to $128 \mu\text{s}$. The dedispersed and downsampled time series are downloaded by the volunteers' computers over the internet and coherently searched for signals from pulsars in circular orbits longer than 11 minutes. A detection statistic, the significance $\mathcal{S} = -\log_{10}(p)$, is evaluated on a grid of parameter space points, where p is the false-alarm probability of the signal in Gaussian noise. A list of the 100 most significant candidates for each dedispersed time series is returned. After completion of all work units for a given observation, the results are post-processed on servers in Hannover, visually inspected and optimized using tools from the PRESTO software package and finally uploaded to a central database at Cornell. A more detailed account of the Einstein@Home pipeline is available in B. Allen et al. (2011, in preparation).

The 20.7 ms pulsar J1952+2630 was found with a maximum significance of $\mathcal{S} = 39.6$ by visual inspection of the Einstein@Home results from a 268 s survey pointing with beam center at equatorial coordinates (J2000.0) $\alpha = 19^{\text{h}}52^{\text{m}}34^{\text{s}}.5$, $\delta = +26^\circ 31' 14''$. The pulsar is detected most significantly at a DM of 315.4 pc cm^{-3} . The NE2001 model of Cordes & Lazio (2002)

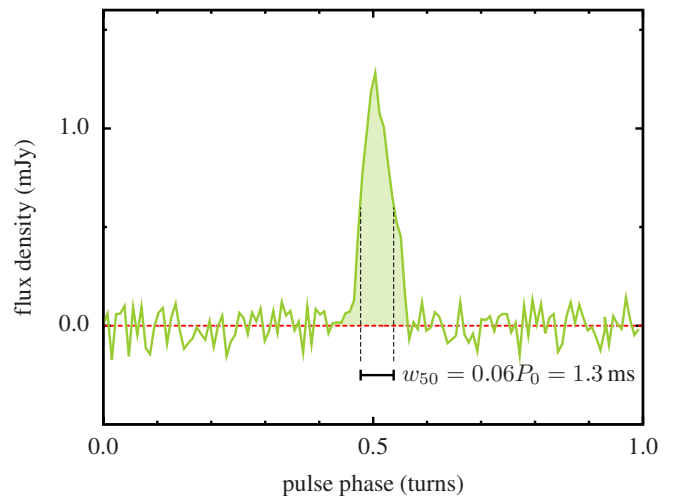


Figure 1. Folded pulse profile of PSR J1952+2630 at 1.4 GHz from the 576 s follow-up observation on 2010 September 20. The resulting period-averaged flux density is $70 \mu\text{Jy} \leq S_{1400} \leq 100 \mu\text{Jy}$ (depending on the precise pulsar position within the beam). The duty cycle is 6% of the pulsar period P_0 . The dispersive delay across a frequency channel is 0.3 ms.

with the given sky position implies a distance of $9.4^{+2.1}_{-1.4}$ kpc. The discovery observation exhibits a marginally significant, but large, barycentric period derivative $\dot{P} = 1.1(7) \times 10^{-9} \text{ s s}^{-1}$ over the short observation time and indicates that PSR J1952+2630 is in a short-period binary system.

3. FOLLOW-UP OBSERVATIONS

To obtain the orbital parameters of the binary system, follow-up observations with the Arecibo telescope were carried out between 2010 July 29 and 2010 November 24. They were conducted mostly in coincidence with PALFA survey observations and used the central beam of the ALFA receiver with the Mock spectrometers.²⁸ These observations provide a total spectral range of 300 MHz in two overlapping bands of 172 MHz with 512 channels each, centered on 1.4 GHz at a time resolution of $65.476 \mu\text{s}$. For our analysis, we use data from the upper band ranging from 1.364 GHz to 1.536 GHz, since the lower band tends to show more radio frequency interference from terrestrial sources. Most follow-up observations cover an observation time $T_{\text{obs}} \approx 600$ s, though a few are of shorter duration. On 2010 July 29 and 2010 July 30 two longer ($T_{\text{obs}} \approx 4200$ s) follow-up observations with a time resolution of $142.857 \mu\text{s}$ covering the same frequency range in 2048 channels were carried out. The epochs of the follow-up observations range from MJDs 55407 to 55525.

On 2010 August 19, gridding observations of the pulsar position were performed at 2.1 GHz to improve the uncertainty of the discovery sky position. We used a square grid centered on the discovery position with nine observation pointings. The pulsar was found with equal signal-to-noise ratio in two of the gridding pointings. The improved sky position halfway between these two pointings is $\alpha = 19^{\text{h}}52^{\text{m}}34^{\text{s}}.4$, $\delta = +26^\circ 30' 14''$ with an uncertainty of $\approx 1'$ given by the telescope beam size.

Figure 1 shows the folded pulse profile of PSR J1952+2630 obtained from the 576 s follow-up observation on 2010 September 19. The full width at half maximum duty cycle is 6%, corresponding to a width of the pulse of $w_{50} = 1.3$ ms.

²⁵ <http://www.cv.nrao.edu/~sransom/presto/>

²⁶ <http://einstein.phys.uwm.edu/>

²⁷ <http://www.top500.org/list/2010/11/100>

²⁸ <http://www.naic.edu/~astro/mock.shtml>

Table 1
PSR J1952+2630 Parameters from a Spin-period-based Analysis

Parameter	Value
Right ascension, α (J2000.0)	19 ^h 52 ^m 6 ^a
Declination, δ (J2000.0)	+26°30′ ^a
Galactic longitude, ℓ (deg)	63.25 ^a
Galactic latitude, b (deg)	−0.37 ^a
Distance, d (kpc)	9.4 ^{+2.1} _{−1.4}
Distance from the Galactic plane, $ z $ (kpc)	0.06
Dispersion measure, DM (pc cm ^{−3})	315.4
Period averaged flux density, S_{1400} (μ Jy)	$\leq 100, \geq 70$
FWHM duty cycle (pulse width, w_{50} (ms))	6% (1.3)
Intrinsic barycentric spin period, P_0 (ms)	20.732368(6)
Projected orbital radius, x (lt-s)	2.801(3)
Orbital period, P_{orb} (day)	0.3918789(5)
Time of ascending node passage, T_{asc} (MJD)	55406.91066(7)
Orbital eccentricity, e	$\lesssim 1.7 \times 10^{-3}$ (2σ)
Mass function, f (M_{\odot})	0.15360(1)
Minimum companion mass, m_c (M_{\odot})	0.945
Median companion mass, $m_{c,\text{med}}$ (M_{\odot})	1.16

Notes. Thirty-four measurements of P and \dot{P} between MJDs 55407 and 55525 are used. The numbers in parentheses show the estimated 1σ errors in the last digits.

^a The sky position was obtained from a gridding observation and has an accuracy of 1′ given by the telescope beam size.

The dispersive delay across a frequency channel is 0.3 ms for the given DM, frequency resolution, and central frequency. We calibrate the profile using the radiometer equation to predict the observation system’s noise level. Since the sky position is known to 1′ accuracy, we can only derive limits on the flux density. We obtain a system equivalent flux density S_{sys} of 3.0–3.8 Jy (depending on the precise pulsar position within the beam). The observation bandwidth is 172 MHz, the observation time is 576 s, and the folded profile has $N = 128$ bins; then, the expected off-pulse noise standard deviation used for calibration is 76–98 μ Jy. The estimated period-averaged flux density of the pulsar at 1.4 GHz is $70 \mu\text{Jy} \leq S_{1400} \leq 100 \mu\text{Jy}$ (depending on its position within the beam).

4. SPIN-PERIOD-BASED ORBITAL SOLUTION

We obtain a solution for the orbital parameters based on measurements of the barycentric spin period and spin period derivative. The pulsar’s orbital motion in a binary system causes changes of the apparent barycentric spin frequency over time due to the Doppler effect. For a circular orbit, the barycentric spin period P as a function of the orbital phase $\theta = \Omega_{\text{orb}}(t - T_{\text{asc}})$ measured from the time of passage of the ascending node T_{asc} is given by

$$P(\theta) = P_0(1 + x\Omega_{\text{orb}} \cos(\theta)). \quad (1)$$

Here, $\Omega_{\text{orb}} = 2\pi/P_{\text{orb}}$ is the orbital angular velocity for an orbital period P_{orb} , P_0 is the intrinsic barycentric spin period of the pulsar, and $x = r \sin(i)/c$ is the projected orbital radius in light-seconds. The radius of the pulsar orbit is denoted by r , i is the orbital inclination, and c is the speed of light.

4.1. First Estimates of the Orbital Parameters

For each follow-up observation of length $T_{\text{obs}} \gtrsim 600$ s, we obtain a pair of values, the barycentric spin period P and the spin period derivative \dot{P} , using the PRESTO software package.

For the two longer follow-up observations of $T_{\text{obs}} \approx 4200$ s, we obtain (P, \dot{P}) pairs over seven contiguous stretches of approximately 600 s each. The acceleration is computed from $a = c\dot{P}P^{-1}$, yielding in total 34 (P, a) pairs. We compute the best-fitting orbital parameters by the method in Freire et al. (2001). We find $x = 2.76(4)$ lt-s and $P_{\text{orb}} = 9.3(1)$ hr; numbers in parentheses are estimated 1σ errors in the last digit.

4.2. Refining the Orbital Parameters

The initial set of orbital parameters is extended and refined using the starting values from Section 4.1. We employ least-squares fitting of the full parameter set Ω_{orb} , T_{asc} , x , and P_0 with Equation (1). After convergence of the fit, the parameters are further refined and errors are estimated by Markov Chain Monte Carlo (MCMC) sampling (Gregory 2005) using an independence chain Metropolis–Hastings algorithm with flat proposal density functions in all parameters. Table 1 shows the refined orbital parameters for PSR J1952+2630 obtained in this manner.

This simple model does not take into account the intrinsic spin-down of the pulsar. Fitting for the spin-down rate is not yet possible with the data reported here, because of the degeneracy with an offset in sky position, which itself is not known to high enough accuracy. This effect results in a systematic error of the best-fit results at an unknown level. Future analysis of pulsar phase instead of spin period, will distinguish the spin-down and orbital effects.

Figure 2 shows all measured spin periods P as a function of the orbital phase θ in the upper panel and the residuals in spin period in the lower panel. No clear structure is visible in the residuals and thus no striking evidence of non-zero eccentricity is apparent, justifying the choice of the circular orbit model.

4.3. Upper Limit on Orbital Eccentricity

To set an upper limit on the eccentricity of PSR J1952+2630’s orbit, we use a spin period model based on the ELL1 timing model (Lange et al. 2001) which is suited for orbits with small

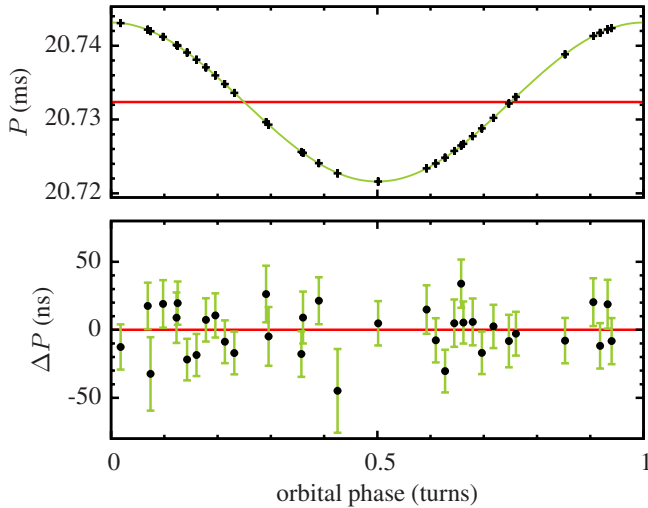


Figure 2. Top: points (with error bars, too small to see) are the measured spin periods P as a function of the orbital phase computed from the orbital model in Table 1. The curve is the expected model spin frequency and the horizontal red line is at P_0 . Bottom: the residual difference between expected and measured spin frequency as a function of the orbital phase. No clear trend indicating non-zero eccentricity is evident.

eccentricity e . Then, Equation (1) in first order in e is modified to

$$P(\theta) = P_0 [1 + x\Omega_{\text{orb}}(\cos(\theta) + \varepsilon_1 \sin(2\theta) + \varepsilon_2 \cos(2\theta))], \quad (2)$$

where the additional constants are given by $\varepsilon_1 = e \sin(\omega)$ and $\varepsilon_2 = e \cos(\omega)$, respectively. The angle ω is the longitude of the periastron measured with respect to the ascending node of the orbit. We now fit for the complete set of parameters ($P_0, x, \Omega_{\text{orb}}, T_{\text{asc}}, \varepsilon_1, \varepsilon_2$). Following the same method as described in Section 4.2, we find the best-fitting orbital solution including the additional eccentricity parameters. MCMC sampling of the parameters space is also conducted for this spin period model (Equation (2)).

The parameters ($P_0, x, \Omega_{\text{orb}}, T_{\text{asc}}$) only change slightly within the confidence regions obtained from the circular fit. The posterior probability distribution function (pdf) of the eccentricity is consistent with a circular ($e = 0$) orbital model; from the posterior pdf we obtain a 2σ upper limit on the eccentricity of $e \lesssim 1.7 \times 10^{-3}$.

5. DISCUSSION

The mass function is defined by

$$f = \frac{4\pi^2 c^3}{G} \frac{x^3}{P_{\text{orb}}^2} = \frac{(m_c \sin(i))^3}{(m_p + m_c)^2}, \quad (3)$$

where m_p and m_c are the pulsar mass and the companion mass, respectively. Inserting the orbital parameters yields $f = 0.15360(1) M_\odot$ for PSR J1952+2630. Assuming a pulsar mass $m_p = 1.4 M_\odot$, we obtain a minimum companion mass $m_c \geq 0.945 M_\odot$ for $i = 90^\circ$. With $i = 60^\circ$ we obtain the median companion mass $m_{c,\text{med}} = 1.16 M_\odot$. For a companion mass $m_c = 1.25 M_\odot$ (smallest measured neutron star mass; Kramer et al. 2006), we obtain an inclination angle of $i = 55^\circ$.

No evidence of eccentricity $e > 1.7 \times 10^{-3}$ is found from this analysis. A common envelope phase with mass transfer in the system's past can explain the almost circular orbit and the short

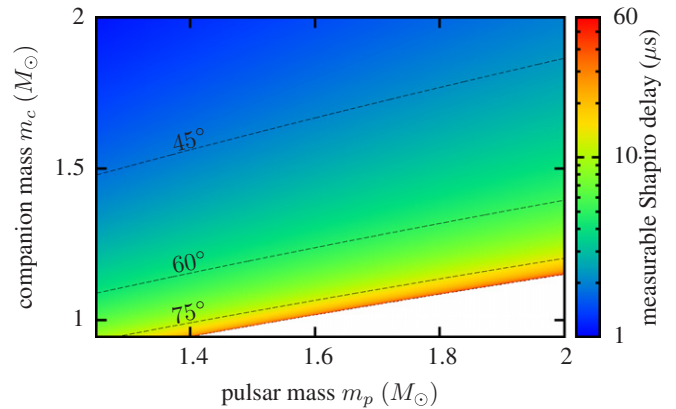


Figure 3. Measurable Shapiro delay amplitude (not absorbed by Keplerian orbital fitting) for PSR J1952+2630 as a function of the pulsar mass and the companion mass. The dashed lines show constant inclination angles of 45° , 60° , 75° , and 90° at the bottom.

orbital period. Also, the companion's progenitor most likely was not massive enough to undergo a supernova explosion; the supernova would have likely kicked the companion which almost guarantees a much higher orbital eccentricity. Thus, a neutron star companion is conceivable but unlikely. The companion most likely is a massive white dwarf. The high white dwarf companion mass, the compactness of the orbit, and the moderate spin period indicate that the pulsar most likely survived a common envelope phase (Ferdman et al. 2010).

Low eccentricity, spin period, and high companion mass most likely place this system in the rare class of intermediate-mass binary pulsars (IMBPs; Camilo et al. 2001). The distance of PSR J1952+2630 to the Galactic plane, $|z| \approx 0.06$ kpc, is comparable to that of the other five IMBPs (Ferdman et al. 2010); this low scale height of the known IMBP population might be due to observational selection effects from deep surveys along the Galactic plane (Camilo et al. 2001).

Phinney (1992) derived a relation between the orbital period and eccentricity of low-mass binary pulsars (LMBPs with companion mass $0.15 M_\odot \lesssim m_c \lesssim 0.4 M_\odot$). Figure 4 in Camilo et al. (2001) displays this relation for LMBPs and IMBPs. The LMBPs follow the theoretically predicted relation very well, while the IMBPs do not follow the same relation; they have higher eccentricities than LMBPs with the same orbital period. The slope, however, seems to be very similar to the one for the LMBPs. This might suggest that there exists a similar relation for this class of binary pulsars. An exact measurement of the orbital eccentricity of PSR J1952+2630 from a coherent timing solution will add another data point that could help to test this hypothesis at short orbital periods.

Detection of the Shapiro delay in PSR J1952+2630 might allow precision mass estimates and strong constraints on the orbital geometry of the binary. Figure 3 shows the measurable Shapiro delay amplitude for PSR J1952+2630 as a function of the pulsar mass and the companion mass; this is the part not absorbed by Keplerian orbital fitting (peak-to-peak amplitude of Equation (28) in Freire & Wex 2010).

Preliminary timing observations using the Mock spectrometers at the Arecibo telescope have time-of-arrival (TOA) uncertainties of approximately $20 \mu\text{s}$. These are currently unconstraining, because no dedicated, deep observations at superior conjunction are available. Observations over a larger bandwidth and use of coherent dedispersion techniques with new instrumentation could improve TOA uncertainties further to $\approx 10 \mu\text{s}$.

Thus, a detection of Shapiro delay requires relatively high inclination angles. If no Shapiro delay is detected, this will enable more stringent lower limits on the companion mass. These alone promise to be interesting, given the already known high minimum companion mass.

6. CONCLUSIONS AND FUTURE WORK

We have presented a spin-period-based analysis of the orbital parameters of the newly discovered binary pulsar PSR J1952+2630. The pulsar has an orbital period of 9.4 hr in an almost circular orbit with a projected radius of 2.8 lt-s. The mass function of $f = 0.154 M_{\odot}$ implies a minimum companion mass of $0.945 M_{\odot}$. Most likely, the companion is a massive white dwarf, although a neutron star companion cannot be excluded.

The above-described observations and further follow-up observations will be used to derive a coherent timing solution for PSR J1952+2630. This will provide a more precisely measured sky position, orbital parameters, and values for the orbital eccentricity and the intrinsic spin-down of the pulsar. This should enable a detailed description of this binary system and constrain its possible formation. A precise position would also enable searches for counterparts in X-ray, infrared, and optical wavelengths, although the large distance makes detections challenging.

Furthermore, detection of Shapiro delay could be possible with further timing observations for high orbital inclinations. Given the already high minimum companion mass derived in this Letter, even a non-detection of the Shapiro delay could provide interesting, more stringent limits on the companion mass and its nature.

This pulsar is the second pulsar discovered by the global distributed volunteer computing project Einstein@Home (Knispel et al. 2010). This further demonstrates the value of volunteer computing for discoveries in astronomy and other data-driven science.

We thank the Einstein@Home volunteers, who made this discovery possible. The Einstein@Home users whose computers detected the pulsar with the highest significance are

Dr. Vitaliy V. Shiryaev (Moscow, Russia) and Stacey Eastham (Darwen, UK).

This work was supported by CFI, CIFAR, FQRNT, MPG, NAIC, NRAO, NSERC, NSF, NWO, and STFC. Arecibo is operated by the National Astronomy and Ionosphere Center under a cooperative agreement with the NSF. This work was supported by NSF grant AST 0807151 to Cornell University. Pulsar research at UBC is supported by an NSERC Discovery Grant and by the CFI. UWM and U. C. Berkeley acknowledge support by NSF grant 0555655. B.K. gratefully acknowledges the support of the Max Planck Society. F.C. acknowledges support from NSF grant AST-0806942. J.W.T.H. is a Veni Fellow of the Netherlands Foundation for Scientific Research (NWO). J.v.L. is supported by EC grant FP7-PEOPLE-2007-4-3-IRG 224838. D.R.L. and M.A.M. acknowledge support from a Research Challenge Grant from WVEPSCoR. D.J.N. acknowledges support by the NSF grant 0647820 to Bryn Mawr College.

REFERENCES

- Abbott, B. P., et al. 2009, *Phys. Rev. D*, **80**, 042003
 Camilo, F., et al. 2001, *ApJ*, **548**, L187
 Cordes, J. M., & Lazio, T. J. W. 2002, arXiv:astro-ph/0207156v3
 Cordes, J. M., et al. 2006, *ApJ*, **637**, 446
 Demorest, P. B., Pennucci, T., Ransom, S. M., Roberts, M. S. E., & Hessels, J. W. T. 2010, *Nature*, **467**, 1081
 Dowd, A., Sisk, W., & Hagen, J. 2000, in ASP Conf. Ser. 202, IAU Colloq. 177, Pulsar Astronomy—2000 and Beyond, ed. M. Kramer, N. Wex, & R. Wielebinski (San Francisco, CA: ASP), 275
 Ferdman, R. D., et al. 2010, *ApJ*, **711**, 764
 Freire, P. C., Kramer, M., & Lyne, A. G. 2001, *MNRAS*, **322**, 885
 Freire, P. C. C., & Wex, N. 2010, *MNRAS*, **409**, 199
 Gregory, P. C. (ed.) 2005, Bayesian Logical Data Analysis for the Physical Sciences: A Comparative Approach with ‘Mathematica’ Support (Cambridge: Cambridge Univ. Press)
 Knispel, B., et al. 2010, *Science*, **329**, 1305
 Kramer, M., & Wex, N. 2009, *Class. Quantum Grav.*, **26**, 073001
 Kramer, M., et al. 2006, *Science*, **314**, 97
 Lange, C., Camilo, F., Wex, N., Kramer, M., Backer, D. C., Lyne, A. G., & Doroshenko, O. 2001, *MNRAS*, **326**, 274
 Phinney, E. S. 1992, *Phil. Trans. R. Soc. A*, **341**, 39
 Stairs, I. H. 2004, *Science*, **304**, 547
 Taylor, J. H., & Weisberg, J. M. 1989, *ApJ*, **345**, 434